Daytime D-region Parameters from Long Path VLF Phase and Amplitude

Neil R. Thomson and Craig J. Rodger

Physics Department, University of Otago, Dunedin, New Zealand

Mark A. Clilverd

British Antarctic Survey, Cambridge, UK

Abstract

Observed phases and amplitudes of VLF radio signals propagating on very long paths are used to validate electron density parameters for the lowest edge of the (D-region of the) Earth's ionosphere at low and midlatitudes near solar minimum. The phases, relative to GPS 1-sec pulses, and the amplitudes were measured near the transmitters (~100-150 km away), where the direct ground wave is dominant, and also at distances of ~8-14 Mm away over mainly all-sea paths. Four paths were used: NWC (19.8 kHz, North West Cape, Australia) to Seattle (~14 Mm) and Hawaii (~10 Mm), NPM (21.4 kHz, Hawaii) and NLK (24.8 kHz, Seattle) to Dunedin, N.Z. (~8 Mm and ~12 Mm). The characteristics of the bottom edge of the day-time ionosphere on these long paths were found to confirm and contextualize recently measured short-path values of Wait's traditional height and sharpness parameters, H' and β, after adjusting appropriately for the (small) variations of H' and β along the paths due to (1) changing solar zenith angles, (2) increasing cosmic ray fluxes with latitude, and (3) latitudinal and seasonal changes in neutral atmospheric densities from the (NASA) MSIS-E-90 neutral atmosphere model. The sensitivity of this long-path (and hence near global) phase-and-amplitude technique is ~±0.3 km for H' and ~±0.01 km^{-1} for β, thus creating the possibility of treating the height (H' ~70 km), as a fiduciary mark (for a specified neutral density) in the Earth's atmosphere for monitoring integrated long term (climate) changes below ~70 km altitude.

1. Introduction

The lowest altitude part of the Earth's ionosphere is the D-region. In this region the neutral atmosphere is ionized mainly by solar EUV radiation and galactic cosmic rays. Low in the D-region, the down-going solar EUV radiation is increasingly absorbed by the increasing atmospheric density; also the electron attachment and recombination rates become so high that the free electron density becomes very small. The lower D-region (~50-75 km) forms the rather stable upper boundary, or ceiling, of the Earth-ionosphere waveguide while the oceans and the ground form the lower boundary. Very Low Frequency (VLF) radio waves (~3-30 kHz) travel over the Earth's surface in this waveguide. Observations of the propagation parameters of these waves result in one of the best probes available for characterizing the height and sharpness of the lower D-region. The (partial) ionospheric reflections of the VLF waves occur because the electron densities (and hence refractive indices) change rapidly (in the space of a wavelength) with height in this region (~50-75 km) typically from less than ~1 cm^{-3} up to ~1000 cm^{-3}, near midday. These electron densities are not readily measured by means other than VLF. Reflected amplitudes of higher frequency radio signals, such as those used in incoherent scatter radars, tend to be too small and so are masked by noise or interference. **The air density at these heights is too high for satellites, causing too much drag, but too low for balloons, providing too little buoyancy.** Rockets are expensive and transient; although some have given good results, there have generally been too few to cope with diurnal, seasonal and latitudinal variations.

Because VLF radio waves penetrate some distance into seawater and, because they can be readily detected after propagating for many thousands of km, the world's great naval powers maintain a number of powerful transmitters to communicate with their submarines. The phase and amplitude of the received signals provides a good measure of the height and sharpness of the lower edge of the D-region. The US Naval Ocean Systems Center (NOSC), developed the two computer programs, **'ModeFinder' (also known as 'MODESRCH' or 'MODEFNDR'), and 'LWPC' ('Long Wave**

Propagation Capability') which take the input path parameters, calculate appropriate full-wave reflection coefficients for the waveguide boundaries, and **search for those modal angles which give phase changes of integer multiples of 2π across a full traverse of the guide (both up and down, after reflection from both upper and lower boundaries)***,* taking into account the curvature of the Earth [e.g. *Morfitt and Shellman,* 1976; *Ferguson and Snyder*, 1990]. Further discussions of the NOSC waveguide programs and comparisons with experimental data by the US Navy and others can be found in *Thomson* [1993, 2010], *McRae and Thomson* [2000, 2004], and references therein.

The NOSC programs can take arbitrary electron density versus height profiles supplied by the user to describe the D-region profile and thus the ceiling of the waveguide. However, from the point of view of accurately predicting (or explaining) VLF propagation parameters, this approach effectively involves too many variables to be manageable in our present state of knowledge of the D-region. As previously, we follow the work of the NOSC group by characterizing the D-region with a "Wait ionosphere" defined by just two parameters, the 'reflection height', H', in km, and the exponential sharpness factor, β, in km^{-1} [*Wait and Spies,* 1964]; the studies referenced in the previous paragraph also found this to be a satisfactory simplification.

Daytime propagation is rather stable, potentially resulting in well-defined values of H' and β characterizing the lower D-region. ModeFinder and LWPC allow users to supply appropriate values of H' and β to determine the amplitude and phase changes along the path and so compare with observations. For the short (~300 km) low-latitude path, from NWC to Karratha, on the coast of N.W. Australia (~20°S geographic, ~30°S geomagnetic, see Figure 1), *Thomson* [2010] used VLF observations plus ModeFinder to determine H' = 70.5 km and β = 0.47 km^{-1} near midday in late October 2009 (i.e. with the **Sun** near the zenith). Similarly, for the short (~360 km) high-midlatitude path, NAA (Maine, USA) to Prince Edward Island, Canada (~46°N geographic, ~53.5°N geomagnetic), *Thomson et al.* [2011] used VLF observations plus ModeFinder to determine H' = 71.8 km and β = 0.34 km^{-1} near midday in June/July 2010 (i.e. with the **Sun** again near the zenith). The lower β at the higher latitude site was attributed to the much higher galactic cosmic ray fluxes at higher latitudes and **enabled a tentative plot of β** versus geomagnetic latitude to be produced.

In the current study here, we use phase and amplitude changes observed along very long near all-sea paths to check on and, to some extent improve on, these values of H' and β. The short paths were needed to measure variations (particularly in β) with latitude. However, although considerable effort was used to try to have these short paths as near all-sea as possible (and hence avoid the considerable uncertainties of land, particularly its low conductivity), the reality is that all the available transmitters are on land. Receiving is also done much more conveniently on land. For modeling purposes, both the low-latitude short path and the high-midlatitude short path were treated essentially as all-sea on the assumption that the parts of the paths that were over land were close (~10 km) to the sea and so likely to have near sea-conductivities. The use of long, nearly all-sea paths used here enables this previous nearly all-sea assumption for the short paths to be checked and validated, because the proportion of the path over land on the long paths here is not only much lower but also the bulk of the paths are far from land (unlike the short paths which tend to pass along and close to coastlines even when over the sea).

Of course, a disadvantage of long paths (in contrast to short paths) is that allowance needs to be made for changes in some of the waveguide parameters along the length of the path. LWPC and ModeFinder generally give very similar results but, because LWPC is set up to automatically take into account changes in the geomagnetic dip and azimuth along the path, it is used for the long paths here. Changes in H' and β due to changing solar zenith angle along the path can be found from *Thomson* [1993] and *McRae and Thomson* [2000], while changes in β due to changing geomagnetic latitude can now also be allowed for from the plot in *Thomson et al.* [2011] mentioned above. Changes in H' with latitude and season depend effectively on the height changes of a fixed neutral density near 70 km altitude and can be estimated from the MSIS-E-90 neutral atmospheric density model [http://omniweb.gsfc.nasa.gov/vitmo/msis_vitmo.html]. Thus it is only now that we are able to make a detailed study of long paths where propagation conditions vary significantly with distance along the path. A clear advantage of long paths (in addition to being able to have a very low proportion of land) is that not only are there much greater phase and amplitude changes along such paths, thus increasing the sensitivity, but also there is much better global averaging along such paths thus giving more potential to measure long term effects, such as those due to global warming, with a higher sensitivity.

2. VLF Measurement Technique and Paths

2.1 The Portable VLF Loop Antenna and Receiver

The phases and amplitudes of the VLF signals were measured both near and far from the transmitters with a portable loop antenna with battery-powered circuitry. The phases were measured (modulo half a cycle) relative to the 1-s pulses from a GPS receiver built in to the portable VLF circuitry. The VLF signals came from NWC (North West Cape, Australia, 19.8 kHz), NPM (Oahu, Hawaii, 21.4 kHz) or NLK (Seattle, 24.8 kHz) which, as for other US Navy VLF transmitters, are modulated with 200 baud MSK. Details of the portable loop and its phase and amplitude measuring techniques are given in *Thomson* [2010]. As previously, for measurements **at less than about 200 km** from the transmitters, the loop had extra resistance (typically 2 x 750 Ω or 2 x 2kΩ) added in series with it to reduce the gain. For all other measurements (far from the transmitters) this series resistance was a nominal 2 x 39 Ω. All phases (and amplitudes) reported here were either measured with 2 x 39 Ω or adjusted to 2 x 39 Ω as in *Thomson* [2010]. The portable loop phase and amplitude measurements used here were made on reasonably flat ground, away from significant hills, with most being made in public parks or by the sides of (minor) roads. Care, as always, was needed to keep sufficiently away from (buried/overhead) power lines and the like, particularly checking that measurements were self-consistent over distances of at least a few tens of meters and from one (nearby) site to the next. Some sites tried needed to be rejected but most, provided certain parts were avoided, proved satisfactory and convenient.

2.2 The Fixed VLF Recorders

NWC, NPM and NLK, like other US Navy VLF transmitters, typically have very good phase and amplitude stability. However, as with the other US transmitters, they normally go off-air once a week for 6-8 hours for maintenance. On return to air, the phase is still normally stable but the value of the phase (relative to GPS or UTC) is often not preserved. In addition, in the course of a typical week, there may be some gradual phase drift or a small number of additional times when there are random phase jumps. For meaningful phase comparisons, it was thus very desirable to have a fixed recorder continuously recording while the portable measurements were being made. This was not convenient to do locally in Australia, Hawaii or Seattle but was done near Dunedin, N.Z., where the signal-to-noise ratio is still very good for NWC, NPM and NLK. The two recorders used, for both phase and amplitude, were softPALs [*Dowden and Adams*, 2008] using two independent VLF receivers and antennas (one loop and one vertical electric field) and GPS 1-s pulses as their phase references. These recorders are part of the Antarctic-Arctic Radiation-belt Dynamic Deposition VLF Atmospheric Research Konsortium (AARDDVARK) [*Clilverd et al.*, 2009] (http://www.physics.otago.ac.nz/space/AARDDVARK_homepage.htm). Because of the stability of the (daytime) propagation this provided a satisfactory method of recording, and compensating for, transmitter phase drifts (or jumps).

2.3 The Paths

Figure 1 shows the locations of the NWC, NPM and NLK transmitters (diamonds), the principal receiving locations (circles) and the great circle propagation paths (GCPs) which, as can be seen, are mainly over the sea. The direction of propagation for each path is indicated by an arrow on its GCP.

3. NWC to Tumwater (near Seattle)

3.1 Measurements of NWC at Tumwater

Around 20 sets of portable loop phase and amplitude measurements of NWC signals were made in and around Tumwater, WA (near Seattle, USA), over the 5 days 5-9 August 2008. Nearly all the measurements were made **during the period ~0000-0230 UT, i.e., within ~2 hours of midday for the path midpoint of the NWC-Tumwater path**. Five sites were used, mainly in public parks, within ~2-12 km of each other. All the phase measurements were entered into an (Excel) spreadsheet together with the site locations measured by a portable GPS receiver and later checked against Google Earth. The spreadsheet was used to adjust the measured phase delays for the different ranges from the transmitter (1.0 μs per 300 m) to allow comparison of sites. All the chosen sites gave satisfactory results: on each of the 5 days the deviation from the mean phase of the (typically) 4 sites used that day was ~±0.5 μs (maximum ~±0.8 μs). The results from the site in Pioneer Park, Tumwater, looked to be the most representative and reliable, and are shown in Table 1.

As previously [*Thomson*, 2010], all phase and amplitude measurements were taken in pairs: first with the loop pointing directly 'towards' the transmitter and then, after rotation by 180^o about the vertical, pointing directly 'away' from the transmitter, thus reversing the phase of the magnetic field but not the phase of any (unintentional residual) electric field. The two resulting amplitude measurements in each pair seldom differed by more than ~0.3 dB, usually less; similarly, the two resulting phase measurements in each pair seldom differed by more than ~0.5 μs, usually less. For each day, the table shows the average of the two 180^o loop orientations for each of the two (sideband) frequencies.

The second last column of the table shows the phase of NWC recorded at Dunedin as shown in Figure 2a. The last column shows the Dunedin phase (in degrees) adjusted in line with the phases of NWC observed at Tumwater as shown in columns 3 and 4. For example, the mean Tumwater phase on 5 Aug 08 was (21.3 + 19.8)/2 **μs** = 20.55 μs, while on 7 Aug 08 it was (17.0 + 15.6)/2 **μs** = 16.3 μs. This (apparent) decrease in phase delay of 20.55 – 16.3 **μs** = 4.25 μs from 5 to 7 Aug 08 is equivalent to an increase of the phase angle by 4.25 $\mathbf{x\ 10^{-6}}$ x 19800 x 360^{o} = 30^{o}; thus the "deg adj." for 7 Aug 2008 relative to 5 Aug is 126^{o} - 30^{o} = 96^{o} as shown. From this last column of Table 1, it can be seen that the range of scatter for the measured phases for the (14.2 Mm) NWC to Tumwater path (relative to the NWC-Dunedin phases) is 18^{o} or ~±9^{o} from the mean, implying a likely random error of ~±4^{o} for the mean of the NWC phase at Tumwater measured over the 5 days, 5-9 August 2008.

3.2 Observations and Modeling: NWC to Tumwater

In a very similar manner to Table 1 here, Table 1 of *Thomson* [2010] showed the phases of NWC measured with the same portable loop system at Onslow, Western Australia, ~100 km ENE over the sea from NWC for the 3 days 21-23 October 2009. From these two tables, the mean Onslow and Tumwater phases (19.3 μs and 17.6 μs) and their corresponding Dunedin phases (-26^{o} and 117^{o}) were then used, in Table 2 here, to find the observed phase delay difference between Onslow and Tumwater. This, of course, required correcting for the phase changes at NWC (as measured at Dunedin) between the times of the Onslow and Tumwater measurements as shown in Table 2.

This delay difference (between Onslow and Tumwater) can be thought of as consisting of two parts: the free space part along the surface of the Earth and the ionospherically reflected part. Indeed programs such as ModeFinder and LWPC output their phases relative to the free-space delay. Table 3 shows the locations of NWC and the principal sites used in each of Tumwater and Onslow (using Google Earth and a portable GPS receiver). The distances in rows 2 & 3 were calculated using the Vincenty algorithm [*Vincenty*, 1975; www.ngs.noaa.gov/cgi-bin/Inv_Fwd/inverse2.prl; www.ga.gov.au/geodesy/datums/vincenty_inverse.jsp] and from these the delays were found using the (exact) speed of light, c = 299.792458 m/μs. The difference between the NWC-Tumwater and

NWC-Onslow delays, 47148.30 μs, was then reduced by an integral number of half cycles: 47148.30 – 1867 x 0.5/0.0198 **μs** = 1.84 μs, to allow for the phase measuring half-cycle ambiguity. This free space delay, modulo half-a-cycle, was then subtracted from the observed delay giving the waveguide part of the delay difference between Onslow and Tumwater, 18.4 – 1.84 **μs** = 16.6 μs ≡ 118°, which was then subtracted from the 128° calculated by LWPC (using H' = 71.7 km and β = 0.43 km^{-1}) for the phase of NWC at Onslow in early August giving 10°, or equivalently 10° - 180° = -170° (due to the half cycle ambiguity) as a preliminary value for the 'observed' phase at Tumwater shown in Figure 2c. This preliminary phase value needs some seasonal refinement because of the different time of year that the measurements were made; the phases of NWC measured at Onslow (near NWC) during late October 2009 need to be adjusted to early August 2008 (when the Tumwater phases were measured) using NWC phases measured in Dunedin because this (5.7 Mm) NWC-Dunedin path will have undergone some seasonal changes in its phase delay in the 2.5 months between early August and late October. (The solar cycle changes will be minimal because both 2008 and 2009 were at solar minimum.)

Fortunately these seasonal phase changes for the NWC-Dunedin path over these 2.5 months can be fairly readily estimated. There are two principal effects. The first is changing H' and β, due to changing solar zenith angle over the period, the values for which were taken from *McRae and Thomson* [2000] and used in LWPC showing that a phase advance of 20° at Dunedin would be expected from early August to late October (mainly due to the decreasing solar zenith angle allowing the **Sun's** Lyman-α to penetrate deeper and so lower H'). The second effect is due to the warming of the neutral atmosphere as the southern-hemisphere season advances from winter towards summer, resulting in the height of a fixed atmospheric density (say 10^{21} m^{-3}) increasing and so H' increasing by the same amount. Neutral number density height profiles (for [N_2]) were found from the MSIS-E-90 atmosphere model (http://omniweb.gsfc.nasa.gov/vitmo/msis_vitmo.html), around 70 km altitude in early August and late October from which it was found that H' increased, due to this warming effect, by an average of ~1.35 km over the length of the NWC-Dunedin path during this period (see Figure 3, discussed later). Using LWPC to model the effect of this 1.35 km height increase (without change in β) shows the phase at Dunedin would decrease by 22° due to this effect alone. The combination of these two effects means that phases in Dunedin in late October are to be expected to be just 22° -20° = 2° lower than in early August (for constant phase at NWC). A similar calculation shows the phase at Onslow would be ~3° higher in late October than in early August, due to these same two effects. This results in the preliminary -170° for the 'observed' phase at Tumwater found above becoming -170° + 2° + 3° = -165°.

The phase of NWC at Onslow was also measured on the 3 days 26-28 June 2008 [*Thomson*, 2010] just ~6 weeks before the Tumwater measurements, while recordings were being made in Dunedin. These June measurements have the advantage over the October Onslow measurements used above in that the predictable changes in the propagation (phase) on the NWC-Dunedin path over this winter 6 weeks due to solar zenith angle (LWPC: ~4^o) and neutral temperature (MSIS-E-90: ~5^o) are much less than for the 2.5 months between August and October (20^o and 22^o respectively from above). Unfortunately the NWC-Dunedin propagation path was less stable 26-28 June 2008 (than in, say, October) as is not unusual in mid-winter. The phase angles at Dunedin over the 3 measurement days in June (when the phase of NWC itself was very stable) covered a range of 28^o (±14^o) as compared with a range of only 2^o in October (relative to a fixed phase at NWC or Onslow). Using the same process for adjusting the June Onslow phases from Dunedin recordings (not shown here) and with the same method of propagation corrections as for October (but now for June), the 'observed' phase at Tumwater in early August 2008 was estimated to be -164^o + 4^o - 5^o = -165^o, essentially the same as was obtained above by adjusting from the October measurements. Hence this -165^o is shown in Figure 2c as the (final) 'observed' phase of NWC at Tumwater for comparison with modeling. The error in the mean 'observed' phase via the June Onslow phases will be largely due to the NWC-Dunedin propagation uncertainties and so ~±10^o (i.e. somewhat less than the ±14^o total measurement range noted above) while the error in the mean via the October Onslow phases will be largely due to uncertainties in the NWC-Dunedin propagation changes between early August and late October, probably ~±7°. Hence the error in the (final) 'observed' phase of NWC at Tumwater of -165° can be estimated to be ~±6°.

The mean amplitude of the NWC signal measured at the Tumwater sites (14.2 Mm from NWC) at **mid-path midday (i.e. midday at the path midpoint)** on the five measurements days, 5-9 August 2008, was 458 μV/m ≡ 53.2 dB above 1 μV/m. Virtually all of the measurements were within ±1 dB of this value. (As can be seen in Figure 2b, NWC's amplitude at Dunedin was steady during this time.) There was significant atmospheric noise near Tumwater but the overall error in the mean amplitude at Tumwater is likely to be **less than approximately** ±0.7 dB. The mean amplitude of the NWC signal measured at Onslow, 21-23 October 2009, was 99.7 dB > 1 μV/m which indicates that NWC was radiating about 0.3 dB below 1 MW [*Thomson*, 2010]. (The same radiated power was also obtained from portable loop measurements in Onslow, 26-28 June 2008.) In Figure 2d the LWPC calculated amplitudes for the various values of *H'* and β are for a radiated power of 1 MW (being a convenient nomalized value) but, to compensate for the apparently 0.3 dB lower radiated power, the 'observed' amplitude is shown as 53.2+0.3 = 53.5 dB > 1 μV/m (being the amplitude which would have been observed at Tumwater had NWC been radiating a full 1 MW).

It can thus be seen from the comparison between calculations and observations for the 14.2 Mm path NWC to Tumwater, in Figures 2c and 2d, that the best fit is for an ionosphere with H' = 71.1 km and β = 0.42 km^{-1} averaged along this solar minimum path.

3.3 Comparison with earlier Measurements and Modeling

These average observed values of H' = 71.1 km and β = 0.42 km^{-1} for the long NWC-Tumwater path can usefully be compared with the values H' = 70.5 km and β = 0.47 km^{-1} for the short (300 km) low-latitude (~30° geomagnetic) NWC-Karratha path (for near overhead **Sun**) [*Thomson*, 2010] and the values *H′* = 71.8 km and β = 0.34 km^{-1} for the short (360 km) high-midlatitude (~53.5° geomagnetic) NAA-PEI path (for near overhead **Sun**) [*Thomson et al.*, 2011]. The latter paper also gives a graph of β versus geomagnetic latitude interpolated using the known latitudinal variation of galactic cosmic ray fluxes. From this graph it can be seen that $\beta \approx 0.485$ km^{-1} for the first 2/3 of the NWC-Tumwater path (~±30° geomagnetic) while the latter 1/3 (at the Tumwater/Seattle end) would have β varying between 0.47 and 0.34 km^{-1} probably averaging about 0.41 km^{-1} thus implying an average β for the path of 0.485 x 2/3 + 0.41 x 1/3 = 0.46 km^{-1} for midday **Sun** at all points along the path. By using the plot of β versus solar zenith angle given (from observations) by *McRae and Thomson* [2000] it can readily be estimated that the average value of β along the path will be lower by about 0.04 km^{-1} (due to the higher solar zenith angles near the NWC and Tumwater ends of the path, even at **mid-path midday**) and so, based on the recent short-path results above, the expected average β would be 0.46 - 0.04 = 0.42 km^{-1} in close agreement with the direct results presented in Figure 2d.

As noted earlier and in *Thomson* et al. [2011], the principal source of variation in height, *H′*, with latitude and season seems to result from the changes in height of a fixed number density (e.g. 10^{21} m^{-3}) in the neutral atmosphere which, as mentioned earlier, can be obtained from the MSIS-E-90 model. This model was used to find the neutral density (actually $[N_2]$, the number density of N_2) at a height equal to *H′* = 70.5 km at the latitude of the (300-km) NWC-Karratha path in late October (2009) when this value of *H′* = 70.5 km was measured. This number density was $[N_2] = 1.31 \times 10^{21}$ m^{-3}. MSIS-E-90 was then used to find the height of this value of $[N_2]$ at other latitudes and times thus giving reasonable estimates for the values of *H′* (for near overhead **Sun**) for those times and places. These values of *H′*, as a function of latitude for early August (2008), are shown in Figure 3, as black squares, together with the baseline result, *H* = 70.5 km, for late October (2009) near NWC (red diamond and horizontal red dotted line). Figure 3 implies (black dashed line) that for early August the (average) value of *H′*, between 22° S and 30° N (i.e the first ~60% of the NWC-Tumwater path) is

70.15 km. For the remaining 40% of the path (latitudes 30°-47° N) the average value of H' can be seen to be (70.3+71.1)/2 = 70.7 km. Thus the average for the whole path from this plot in Figure 3 (i.e. for midday at all points on the path) is $H' = 0.6 \times 70.15 + 0.4 \times 70.7 = 70.37$ km. The actual average H' for the path will be a little higher than this because, at **mid-path midday**, the NWC end will have morning solar zenith angles while the Tumwater end will have afternoon solar zenith angles. These increases of H' with solar zenith angle towards the ends of the (midday) path can be found from the appropriate plot in *McRae and Thomson* [2000]. The average increase in H' for the first ~1/3 of the path (the NWC or morning end) was thus found to be **~1.7 km**. From this same plot, the last ~1/3 of the path (the Tumwater or afternoon end) would also look to have an increase of **~1.7 km**. However, this end is at a significantly higher geomagnetic latitude, and so has a much higher proportion of its electron density from (zenith angle independent) cosmic rays than the *McRae and Thomson* [2000] plot. Hence less variation in H' with solar zenith angle is to be expected at the Tumwater end. A similar latitude situation exists for the path NAA to Cambridge for which amplitude and phase plots were available [*Thomson et al.*, 2007] allowing LWPC to be used to find changes in H' with solar zenith angle for this high-midlatitude path. It was thus found that the average increase in H' for the afternoon 1/3 of the NWC-Tumwater would likely be only ~0.8 km. Hence the (final) value of H', averaged along the NWC-Tumwater path (at *mid-path midday*), from all these earlier observations would be $H' = 70.37 + (1.7 + 0.8)/3$ km = 71.2 km. This is only ~0.1 km higher than the 71.1 km obtained from the present direct measurements on the NWC-Tumwater path shown in Figure 2c which is thus very satisfactory. **These comparisons between the long-path measurements of H' and β with the corresponding values from short-path results adjusted for changing solar zenith angle and changing latitudes along the path are summarized in Table 4 (columns 2 and 3).**

4. NPM (Hawaii) to Dunedin, NZ

Measurements similar to those for the NWC to Tumwater path were also made for the ~8.1 Mm NPM to Dunedin path. The US Navy 21.4 kHz transmitter, NPM (on the Hawaiian Island of Oahu), is located at 21.4202° N, 158.1511° W. Phases and amplitudes of NPM were measured with the portable loop system at several suitable sites on the eastern side of the nearby island of Kauai, on the four days 27, 28, 30 and 31 Oct 2009 (NPM was off-air for ~8 hours until ~02 UT on 29 Oct 2009). The prime receiving site there (which gave readings consistent with those at the other sites on Kauai) was in Lydgate Park located at 22.0385° N, 159.3362° W, which was thus 140.42 km from NPM (using the **Vincenty** algorithm). Phase and amplitude recordings of NPM were made at Dunedin (using softPAL recorders) before, during and after the Kauai measurements. Portable loop measurements of NPM's phase and amplitude were made at several sites in Dunedin (giving good mutual agreement) both before and after the Kauai measurements. The prime (reference) site in Dunedin was in Bayfield Park at 45.8938° S, 170.5236° E which, using the **Vincenty** algorithm, is thus 8098.08 km from NPM. The path difference between Bayfield Park and Lydgate Park was thus found to be 8098.08 - 140.42 **km** = 7957.65 km which, using the (exact) speed of light, corresponds to a free-space delay of 26543.87 μs which, modulo half-a-cycle of NPM's 21.4 kHz (i.e. 0.5/0.0214 μs) becomes 1.81 μs. The corresponding observed phase delay (from the portable loop phase measurements in Bayfield and Lydgate Parks) was found (in a similar manner to that for NWC and Tumwater in Section 3) to be 5.2 μs, which means the "waveguide only" part of the delay was 5.2 - 1.8 μs = 3.4 μs, **modulo a quarter of a period of 21.4 kHz, because the 21.4 kHz phase measurement is derived from the (portable loop) 21.35 kHz and 21.45 kHz sideband measurements, either or both of which have (independent) half-cycle ambiguities**. This "waveguide only" delay of 3.4 μs ≡ 26° (modulo 90°) is then subtracted from the 127° phase found by LWPC (using H' = 71.8 km and β = 0.44 km^{-1}) for NPM at Lydgate in October to get the 127° - 26° - 90° = 11° shown as the "observed" phase for NPM at

Dunedin in Figure 4 which also shows the LWPC-calculated phases for NPM at Dunedin for appropriate values of H' and β.

The mean amplitude of the NPM signal measured at the Dunedin sites (~8.1 Mm from NPM) at **mid-path midday** (~23 UT) in October/November 2009 was 460 μV/m ≡ 53.3 dB above 1 μV/m which is shown as the "observed" amplitude in Figure 4 for comparison with LWPC modeling. Virtually all of the measurements were within ±0.7 dB of this value so that the error in the mean is likely to be ~±0.5 dB. On Kauai, ~140 km from NPM, the measured effective midday mean amplitude of the NPM signal, 27-31 Oct 2009, was 40.6 ±2 mV/m ≡ 92.2 dB > 1 μV/m. Using LWPC, with an appropriate (midday, late October, 22º N) ionosphere, H' = 71.8 km, β = 0.44 km^{-1}, on this NPM-Kauai path, gave the radiated power as 375 kW. This power was then used again in LWPC to calculate the expected amplitudes of NPM at Dunedin (8.1 Mm away) for appropriate values of H' and β giving the results shown in Figure 4.

From Figure 4 it can be seen that H' = 70.8 km and β = 0.46 km^{-1} give good fits to the observed phases and amplitudes for NPM-Dunedin. These average observed parameters for this fairly long path can again usefully be compared with the recent short-path parameters as was done for NWC-Tumwater in Section 3.3. **A summary is given in Table 4 (columns 4 and 5).** Because the NPM-Dunedin path is much shorter (8.1 Mm compared with 14.2 Mm) and more North-South (covering less local time), the variations in H' and β along the path are much smaller, but can be dealt with in a very similar manner. For the ~70% of the NPM-Dunedin path with low geomagnetic latitudes between 21º N and 30º S, the average β (as before) will be ~0.485 km^{-1}, while for the remaining 30% of the path (the Dunedin end) the average β will be (0.47+0.34)/2 km^{-1} = 0.41 km^{-1} giving β = 0.7 x 0.485 + 0.3 x 0.41 km^{-1} = 0.463 km^{-1} for the path average, for the **Sun** near the zenith all along the path. The effects of the actual higher solar zenith angles near the ends of the path (at **mid-path midday**) can be estimated, as before, from *McRae and Thomson* [2000], as reducing β by ~0.006 km^{-1} thus giving β = 0.463-0.006 km^{-1} = ~0.46 km^{-1} which agrees very well with the 0.46 km^{-1} directly measured here on the long NPM-Dunedin path. From the green lines in Figure 3, the average value of H' (for near overhead **Sun**) for the NPM-Dunedin path (21º N to 46º S, late October) is 70.55 km. From *McRae and Thomson* [2000], the small increases in H' near the ends of the path (due to the higher solar zenith angles there at **mid-path midday**) can be estimated (as for the NWC-Tumwater path in section 3). This resulted in $H' = 70.55 + 0.25$ km = 70.8 km which again agrees very well with the 70.8 km found here from direct observations on the long NPM-Dunedin path.

5. NWC to Kauai, Hawaii

Measurements similar to those for the NWC-Tumwater path were also made for the ~10.6 Mm path NWC to Kauai. Phases and amplitudes of NWC were measured with the portable loop system at several suitable sites on the eastern side of the Island of Kauai on five days, 27-31 Oct 2009. The prime receiving site there (which gave readings consistent with those at the other sites on Kauai) was the same site in Lydgate Park as used for NPM (section 4); this site was 10560.92 km from NWC (again making use of the **Vincenty** algorithm). From section 3.2, Table 2, the distance from NWC to (the prime site in) Onslow was 100.16 km so that the Lydgate-Onslow path difference is 10560.92 - 100.16 km = 10460.76 km which, using the (exact) speed of light gives the free-space delay difference as 34893.35 μs which, in turn, **modulo half-a-period of NWC's 19.8 kHz (0.5/0.0198 μs), becomes 19.6 μs**. As mentioned previously (section 3.2 and *Thomson* [2010]), the phase of NWC was measured with the portable loop system at Onslow, 21-23 Oct 2009. Phase (and amplitude) recordings of NWC were also made at Dunedin (using softPAL recorders) before, during and after these Onslow and Kauai measurements to monitor and correct for any phase changes at NWC during this period. The NWC-Dunedin propagation path was, as usual, very stable during this late spring, solar minimum period making the Dunedin recorders very effective in monitoring the phase changes of the NWC transmitter. With the help of these Dunedin recordings using a very similar procedure to that for the NWC-Tumwater path (in section 3.2), the portable loop measurements at Lydgate Park and Onslow, gave the observed Lydgate-Onslow phase difference (modulo half-a-cycle of NWC) as 19.6 μs. **Subtracting the calculated free-space delay of 19.6 μs (from above) from this observed 19.6 μs then gave 0 μs ≡ 0° or, modulo half-a-cycle, 180°, for the waveguide-only part of the Onslow-Lydgate delay.** Subtracting this 180° from the 131° calculated by LWPC (using H' = 70.5 km, β = 0.47 km^{-1}) for the phase of NWC at Onslow in late October gave -49° which is thus shown as the "observed" phase of NWC at Lydgate Park in Figure 5 where it is compared with the LWPC-calculated NWC phases at Lydgate Park using suitable values of H' and β.

The mean amplitude of the NWC signal measured at the Kauai sites (~10.6 Mm from NWC) at **mid-path midday** (~01 UT) 27-31 October 2009 was 590 μV/m ≡ 55.4 dB above 1 μV/m. Figure 5 shows the LWPC-calculated amplitudes at Kauai for NWC radiating 1 MW. As noted in section 3.2, the Onslow portable loop measurements were more consistent with NWC radiating ~0.3 dB below 1 MW. The "observed" amplitude for NWC is thus shown in Figure 5 as 55.4 + 0.3 dB = 55.7 dB (as would have been observed if NWC had been radiating a full 1 MW).

From Figure 5 it can be seen that H' = 71.0 km and β = 0.46 km^{-1} give good fits to the observed phases and amplitudes for NWC-Kauai. These average observed parameters for this long path can again usefully be compared with the recent short-path values as was done for NWC-Tumwater in Section 3.3 and NPM-Dunedin in section 4. **Again a summary is given in Table 4 (columns 6 and 7).** Because all of the NWC-Kauai path is at low geomagnetic latitudes (between 21º N and 30º S), the average β (as before) would be ~0.485 km^{-1} if the **Sun** were near overhead at all points along the (10.6 Mm) path. The effects of the higher solar zenith angles near the ends of the path (at **mid-path midday**) can be estimated, as previously, from *McRae and Thomson* [2000], as reducing β by ~0.016 km^{-1} thus giving β = 0.485 - 0.016 km^{-1} = ~0.47 km^{-1} which agrees quite well with the 0.46 km^{-1} found above from the directly-measured, long NWC-Kauai path. From Figure 3, the average value of H' (for near overhead **Sun**) for the NWC-Kauai path (22º S to 22º N) is 70.6 km in late October. From *McRae and Thomson* [2000], the small increases in H' near the ends of the path (due to the higher solar zenith angles there at **mid-path midday**) can be estimated (as for the NWC-Tumwater path in section 3). This resulted in H' = 70.6 + 0.55 **km** = 71.15 km which again agrees quite well with the 71.0 km found here from direct observations on the long NWC-Kauai path.

However, unlike the two previously discussed paths here (NWC-Tumwater and NPM-Dunedin), as can be seen in Figure 1, this NWC-Kauai path passes over significant amounts of land; ~1.8 Mm of this ~10.6 Mm NWC-Kauai path is over northern Australia where the (LWPC-built-in) ground conductivity is quite low, ~1 x 10^{-3} S/m. As an example of the sensitivity due to ground conductivity, when the LWPC calculation for NWC-Kauai (with H' = 71.0 km and β = 0.46 km^{-1}) was repeated with an all-sea conductivity, the calculated amplitude at Kauai increased by ~4.3 dB and the phase advanced by ~27°. Given the considerable uncertainties in the ground conductivities, the agreement between the estimated and observed values of β and H' for this NWC-Kauai path is remarkably good.

6. NLK (Seattle) to Dunedin, NZ

Similar measurements for the long ~12.3 Mm, nearly all-sea path NLK (24.8 kHz, Seattle) to Dunedin were also made. NLK is located at 48.2036° N, 121.9171° W (from Google Earth). Phases and amplitudes of NLK were measured with the portable loop system at several suitable sites ~150 km south of Seattle in the vicinity of Olympia/Tumwater WA, USA, 5-9 August 2008. The prime receiving site there (which gave readings consistent with other nearby sites within a few km) was the same site in Pioneer Park (Tumwater) as used in Section 3.2 (Table 3), which is 152.60 km from NLK (using the **Vincenty** algorithm). Phase and amplitude recordings of NLK were made at Dunedin (using softPAL recorders) before, during and after the Tumwater measurements. Portable loop measurements of the phase and amplitude of NLK were made at several sites in Dunedin (giving quite good mutual agreement) both before and after the Tumwater measurements. The prime (reference) site in Dunedin was again in Bayfield Park (as used in Section 4) which, using the **Vincenty** algorithm, is 12315.74 km from NLK. The path difference between Bayfield Park and Pioneer Park was thus found to be

12315.74 - 152.60 **km** = 12163.15 km which, using the (exact) speed of light, corresponds to a free-space delay of 40571.89 μs which, modulo half-a-cycle of NLK's 24.8 kHz (i.e. 0.5/0.0248 μs) becomes 7.37 μs. The corresponding observed phase delay (from the portable loop measurements in Bayfield and Pioneer Parks) was found (in a similar manner to that for NWC and Tumwater in Section 3.2) to be 17.7 μs, which means the "waveguide only" part of the delay was 17.7 - 7.4 **μs** = 10.3 μs ≡ 92°. This 92° was then subtracted from the 127° calculated by LWPC (using H' = 71.7 km, β = 0.33 km^{-1}) for the phase of NLK at Tumwater in early August, giving 35°, or equivalently 35° - 180° = -145° (due to the half cycle ambiguity), for the 'observed' phase at Tumwater shown in Figure 6a which also shows the LWPC-calculated phases for NLK at Dunedin for appropriate values of H' and β.

The mean amplitude of the NLK signal measured at the Dunedin sites (~12.3 Mm from NLK) at **mid-path midday** (~23 UT) in July/August 2008 was 65 μV/m ≡ 36.3 dB above 1 μV/m; this is shown as the "observed" amplitude in Figure 6b for comparison with the LWPC modeling. Nearly all of these measurements were within ±1 dB of this value so that the error in the mean is likely to be ~±0.7 dB. At Tumwater, ~153 km from NLK, the measured effective midday mean amplitude of the NLK signal, 5-9 Aug 2008, was 31.7 ±2 mV/m ≡ 90.0 dB > 1 μV/m. Using LWPC, with an appropriate (midday, early August, 47.5° N) ionosphere, H' = 71.7 km, β = 0.33 km^{-1}, on this NLK-to-Tumwater path, gave the radiated power as 290 kW. This power was then used again in LWPC to calculate the expected amplitudes of NLK at Dunedin (12.3 Mm away) for appropriate values of H' and β giving the results shown in Figure 6b for comparison with the observed amplitude.

As for the other three long paths discussed here (sections 3, 4 and 5), H' and β for this long path can again usefully be estimated from the recently measured short-path parameters. **Again a summary is given in Table 4 (columns 8 and 9).** From Figure 3, the average value of H' (for near overhead **Sun**) for the NLK-Dunedin path (48° N to 46° S, early August) is 70.0 km. From *McRae and Thomson* [2000], the increases in H' near the ends of the path (due to the higher solar zenith angles there at **mid-path midday**) can be estimated (as for the NWC-Tumwater path in section 3.3). This resulted in H' = 70.0 + 0.8 km = 70.8 **km**. For the ~60% of this NLK-Dunedin path with low geomagnetic latitudes between 30º N and 30º S, the average β (as before) will be ~0.485 km^{-1}, while for the remaining 40% of the path (the Seattle and Dunedin ends) the average β will be ~(0.47+0.34)/2 **km^{-1}** = 0.41 km^{-1} giving β = 0.6 x 0.485 + 0.4 x 0.41 **km^{-1}** = 0.455 km^{-1}, for the **Sun** near the zenith all along the path. The effects on β of the actual higher solar zenith angles near the ends of the path (at **mid-path midday**) can be estimated, as before, from *McRae and Thomson* [2000], as reducing β by ~0.02 km^{-1} giving β = 0.455 - 0.02 **km^{-1}** = ~0.435 km^{-1} which does not agree very well with the ~0.38 km^{-1} indicated by the direct observations in Figure 6b. Indeed, as can be seen in Figure 6b, it appears that β = 0.435 km^{-1} would give an observed amplitude at Dunedin of 38.7 dB > 1μV/m whereas the actual portable loop observations gave 36.3 dB at Dunedin.

This apparent discrepancy appears to be a result of the effective radiated power from NLK being somewhat direction dependent. NLK is unusual in that, instead of using very tall towers (400-500 m high) on flat ground to make the antenna high enough to get a reasonable radiation efficiency, it has wires strung between mountain ridges across a valley with the radiating current coming up to these in a cable from the transmitter on the valley floor below [e.g., *Watt*, 1967]. As well as the NLK amplitude measurements near Tumwater (~153 km SSW of NLK), additional amplitude measurements were made over a much greater land area and range of directions ~SW of NLK (the closest to NLK being at Dosewallips State Park, 93 km from NLK, while the furthest was at Westport on the west coast, 220 km from NLK). A range-corrected plot of these measured amplitudes of NLK as a function of azimuth (degrees east of north from NLK) is shown in Figure 6c, where it can be seen that the amplitudes measured at sites in the direction of Dunedin are ~3 dB lower than those measured at sites near Tumwater. As the amplitudes at Tumwater were used to determine the radiated power of 290 kW used for NLK in calculating the amplitudes at Dunedin in Figure 6b, it seems that the low amplitudes (~36 dB) measured at Dunedin may well be due to the lower radiated power in this direction. Thus quite likely the value of β = 0.435 km^{-1} estimated from the earlier short path measurements will be more appropriate than the (radiation-direction compromised) value, β = 0.38 km^{-1}, from amplitude comparisons in Figure 6b. Indeed, if β = 0.435 km^{-1} is used in the NLK-Dunedin phase plot in Figure 6a then this gives H' = 70.9 km in close agreement with the H' = 70.8 km estimated above from the short path parameters.

7. Discussion, Summary and Conclusions

Phases and amplitudes of suitable VLF signals were measured using a portable loop system referenced to GPS 1-second pulses. Observations of the midday VLF radio phase changes and amplitude attenuations along four long, mainly all-sea paths have been presented here: NWC (N.W. Australia) to Seattle (14.2 Mm), NPM (Hawaii) to Dunedin, N.Z. (8.1 Mm), NWC to Kauai, Hawaii (10.6 Mm) and NLK (Seattle) to Dunedin, N.Z. (12.3 Mm). Average values of the height, H', and sharpness, β, of the D-region of the ionosphere along each path were then determined by modeling with the waveguide code, LWPC, so that the modeled phases and amplitudes agreed with those observed.

These resulting average values of H' and β for each of the four long paths were then compared with recent short (~300 km) path measurements of H' and β at (i) a low geomagnetic latitude and (ii) a mid-high geomagnetic latitude. The interpolation of β with geomagnetic latitude along the paths was obtained from these by using the known variation of cosmic ray flux with geomagnetic latitude. The variations (interpolations) of H' with season and geographic latitude along the paths were obtained from the short-path observations by extending them with the MSIS-E-90 neutral atmosphere model. Small additional variations of H' and β due to changes in solar zenith angle near the ends of the paths were estimated from the observations of *McRae and Thomson* [2000]. **Han and Cummer [2010] measured H' near Duke University, ~37° N geographic, in summer using natural lightning.**

Their values of H' for near overhead Sun are typically in the range 71-72 km, averaging ~71.5 km which is a little greater than the H' = 70.9 km from MSIS-E-90 and Figure 3 in June/July here but is quite likely just within the combined experimental errors of the two methods.

For the NPM-Dunedin path (8.1 Mm), both the direct long-path method and the interpolated/extrapolated short-path method gave essentially the same results, H' = 70.8 km and β = 0.46 km^{-1}. The very long (14.2 Mm) NWC-Seattle path gave the same (average) value of β=0.42 km^{-1} with both short- and long-path methods **while the H' = 71.1 km obtained from the long path was only marginally lower, by ~0.1 km (~100 m), than the H' = 71.2 km obtained using the short-path method.** A similar small height difference was also seen on the (10.6 Mm) NWC-Kauai path (H' = 71.0 and 71.15 km) but this is of even less significance because of the uncertainty in the (low) conductivity of the ~1.8 Mm of (Australian) ground on this path. Similarly the difference between the short-path and long-path values of β for this path (0.47 and 0.46 km^{-1}) is also probably not enough to be significant for the same uncertain ground conductivity reason. For the (12.3 Mm) NLK-Dunedin path, in contrast with the two NWC paths, the H' = 70.9 km from the long-path method was slightly higher than the H' = 70.8 km from the short-path method. The uncertainties for β on this path, due to NLK and some of its nearby measurements being undertaken in mountainous terrain, mean that this small difference in H' (0.1 km) is probably not significant for this path.

Overall, the agreement between the short-path and long-path observations is remarkably good with maximum differences of only ~0.15 km in height, H', and 0.01 km^{-1} in sharpness, β. This is suggestive that the errors (~±0.5 km for H' and ~±0.03 km^{-1} for β) for the short-path measurements reported in *Thomson* [2010] and *Thomson et al.* [2011] may have been a little conservative. Because both the transmitters and the measurement sites there were on land, and the paths were short (~300 km), there was a concern that the resulting proportion of low-conducting land and coastal boundaries (though appreciably less than for 50% of the paths) might have been having more effect than hoped. Any concern that this might have been a difficulty is now markedly reduced. The use of the MSIS model for estimating changes in *H′* with season and latitude (but not with solar zenith angle) effectively assumes there are no relevant neutral atmosphere composition changes (near 70 km altitude) with season and latitude. For the cosmic rays, which ionize all atmospheric constituents, this is very likely to be the case. However, for the minor but important constituent NO (ionized by Lyman-α) this is less certain. None-the-less the apparent agreement resulting from using MSIS with this assumption may well be implying the proportion of NO in the neutral atmosphere at heights near 70 km, at least for the low and midlatitudes studied here, is fairly constant with season and latitude.

The validated, quiet-time, daytime modeling presented here provides an improved baseline for measuring a wide variety of perturbations to the lower D-region and hence the Earth-ionosphere waveguide. Such 'perturbations' include the transition from day to night (so improving nighttime parameters [*McRae and Thomson*, 2007, 2009]), the effects of solar flares [e.g., *Thomson et al*., 2005] and the effects of particle precipitation [e.g., *Rodger et al.*, 2007], which can perturb the day or night ionosphere.

Of course, although the modeling by LWPC seems very good, it will not be perfect; better modeling will be found in the future. In particular, the representation of the electron density versus height profile in the lower D-region by the two simple parameters, *H′* and β, though very good, is not likely to be exact. However, the raw phase and amplitude measurements for the long paths measured here are independent of the current modeling; these measurements could well be used in future, improved modeling thus determining (retrospectively) improved values for the height (and sharpness) of the lowest edge of the (D-region of) the Earth's ionosphere. The sensitivity of these long paths to these D-region parameters is quite high; the error of ±6° in phase and ±0.7 dB in amplitude estimated for the 14.2 Mm NWC-Tumwater path in section 3.2 corresponds (using Figure 2) to a sensitivity of less than approximately ±0.3 km in *H′* and ~±0.01 km^{-1} in β. Also, as can be seen from Figure 2c, a (short term) change in height, *H′*, (by say 1 km) while β remained constant, caused by (say) a simple vertical height change in the neutral atmosphere alone (i.e., where the height of a fixed density, say 10^{21} m^{-3}, changes by 1 km) will cause a phase change of ~44° per km. In such a (constant β) case, the long term phase measurement sensitivity of ±6° corresponds to a height sensitivity of ~±0.15 km. For very short term changes over a few hours, sensitivities as low as ±4° or ±0.1 km = ±100 m are likely for this very long path (if β is constant). Over much longer times, when β may not be quite constant, and even without improved modeling, future long-path measurements of H' and β can potentially measure changes in height (of ~0.3 km) over time to a higher accuracy than current modeling can determine absolute height. Clearly such potential observations could include determining H' changes over a solar cycle. It might also be possible to use such height changes (averaged over individual solar cycles), over even longer periods of time, to test theories of global warming and the corresponding height-integrated atmospheric expansions and contractions below a specified height in the D-region, such as H', which corresponds effectively to the (fixed) density level down to which the external ionizing radiations (Lyman-α, galactic cosmic rays etc) penetrate before they are absorbed or their effects are overwhelmed by electron loss processes (attachment/recombination).

Acknowledgements

The authors are very grateful their colleague, David Hardisty, for his design, development and construction of the VLF phase meter. Thanks also to http://rimmer/ngdc.noaa.gov of NGDC, NOAA, US Dept. of Commerce, for the digital coastal outline used in Figure 1.

References

Dowden, R.L., and C.D.D. Adams (2008), SoftPAL, paper presented at the 3rd VERSIM Workshop, Eötvös Univ., Tihany, Hungary, 15-20 Sept.

Ferguson, J. A. and F. P. Snyder (1990), Computer programs for assessment of long wavelength radio communications, version 1.0: full FORTRAN code user's guide, *Naval Ocean Systems Center Tech. Doc. 1773, DTIC AD-B144 839*, Def. Tech. Inf. Cent., Alexandria, Va.

Han, F. and S.A. Cummer (2010), Midlatitude daytime D region ionosphere variations measured from radio atmospherics, *J. Geophys. Res.*, *115*, A10314, doi:10.1029/20010JA015715.

McRae, W. M. and N. R. Thomson (2000), VLF phase and amplitude: daytime ionospheric parameters, *J. Atmos. Sol.-Terr. Phys.,* 62(7), 609-618.

McRae, W. M. and N. R. Thomson (2004), Solar flare induced ionospheric D-region enhancements from VLF phase and amplitude observations, *J. Atmos. Sol.-Terr. Phys.,* 66(1) 77-87.

Morfitt, D. G. and C. H. Shellman (1976), MODESRCH, an improved computer program for obtaining ELF/VLF/LF mode constants in an Earth-Ionosphere Waveguide, *Naval Electr. Lab. Cent. Interim Rep. 77T, NTIS Accession ADA032573*, Natl. Tech. Inf. Serv., Springfield, VA.

Rodger, C.J., M.A. Clilverd, N.R. Thomson, R.J. Gamble, A. Seppälä, E. Turunen, N.P. Meredith, M. Parrot, J.-A. Sauvaud, and J.-J. Berthelier (2007), Radiation belt electron precipitation into the atmosphere: recovery from a geomagnetic storm, *J. Geophys. Res.,* 112, A11307, doi:10.1029/2007JA012383.

Thomson, N. R. (1993), Experimental daytime VLF ionospheric parameters, *J. Atmos. Terr. Phys., 55*, 173-184.

Thomson, N. R., C. J. Rodger and M. A. Clilverd (2005), Large solar flares and their ionospheric *D* region enhancements, *J. Geophys. Res.*, *110*(A6): A06306, doi:10.1029/2005JA011008.

Thomson, N. R., M. A. Clilverd and W. M. McRae (2007), Nighttime ionospheric D-region parameters from VLF phase and amplitude, *J. Geophys. Res.*, *112*(A7): A07304, doi:10.1029/2007JA012271.

Thomson, N. R. and W. M. McRae (2009), Nighttime ionospheric D-region: Equatorial and Non-equatorial, *J. Geophys. Res.*, *114*(A8): A08305, doi:10.1029/2008JA014001.

Thomson, N.R. (2010), Daytime tropical D region parameters from short path VLF phase and amplitude, *J. Geophys. Res.*, *115*, A09313, doi:10.1029/2010JA015355.

Thomson, N.R., M. A. Clilverd and C. J. Rodger (2011), Daytime midlatitude D region parameters at solar minimum from short-path VLF phase and amplitude, *J. Geophys. Res.*, *116*, A03310, doi:10.1029/2010JA016248.

Vincenty, T. (1975), Direct and inverse solutions of geodesics on the ellipsoid with application of nested equations, *Survey Review*, *22(*176), 88-93.

Wait, J.R., Spies, K.P., (1964), Characteristics of the Earth-ionosphere waveguide for VLF radio waves, *NBS Tech. Note 300*, Natl. Bur. of Stand., Boulder, Colo.

Watt, A.D. (1967), *VLF Radio Engineering*, Elsevier, New York.

Figure Captions

Figure 1. The transmitter sites (red diamonds), the receiver sites (blue circles) and the long paths across the Pacific Ocean used for the VLF phase and amplitude measurements.

Figure 2. (a) NWC phases and (b) amplitudes recorded at Dunedin, N.Z., while portable loop measurements of NWC were being made at Tumwater (near Seattle). Comparisons of observed midday (c) phases and (d) amplitudes (using NWC-Dunedin as reference) with modeling by LWPC for the NWC to Tumwater path.

Figure 3. Variations of H' (in km, for near overhead **Sun**) with latitude and season due to neutral atmosphere changes from the MSIS-E-90 atmospheric model. The plots are only slightly longitude dependent. The red diamond and its associated red dotted line are the reference height (H' as measured for the short, 300 km, NWC-Karratha path). The other dotted and dashed lines are used to aid in visualizing the averaging of H' along some of the long paths as discussed in the text.

Figure 4. Comparisons of observed midday phases and amplitudes with modeling for the NPM to Dunedin path.

Figure 5. Comparisons of observed midday phases and amplitudes with modeling for the NWC to Kauai, Hawaii, path.

Figure 6. Comparisons of observed midday (a) phases and (b) amplitudes with modeling for the NLK to Dunedin path plus (c) the observed directivity of NLK towards Dunedin and Tumwater.

Tables

Table 1. NWC Phases Measured at Tumwater, WA, and Dunedin[a]

UT Date	UT	L (µs)[b]	H (µs)[b]	Dn (deg)[b]	adj. (deg)
5 Aug 08	0022	21.3	19.8	103	103
6 Aug 08	0240	21.3	19.8	90	90
7 Aug 08	0027	17.0	15.6	126	96
8 Aug 08	0018	8.7	6.7	197	106
9 Aug 08	0124	24.0	21.8	71	88

[a]The phase measurements at Tumwater were observed using 2 x 39 Ω and are in µs (L = 19.75 kHz, H = 19.85 kHz). Measurements at Dunedin are in degrees. The last column, 'adj.', illustrates the consistency (while NWC's phase drifts) by adjusting the 'Dn' phase in line with the Tumwater 'µs' phase, as explained in the text.
[b]Mean for these ten Tumwater phases is 17.6 µs. Mean for these five phases at Dunedin is 117°.

Table 2. Observed NWC Phase Difference between Tumwater, WA, USA and Onslow, N.W. Australia[a]

Observed	Phase (µs)	Dn (deg)
Tumwater 2 x 39 Ω	17.6	117
Onslow 2 x 39 Ω	19.3	-26
Onslow 2 x 39 Ω	-0.8	117
Δ Phase (Tumwater-Onslow)	18.4	—

[a]The observed phase difference between Tumwater and Onslow (row 4), after correcting the measured Onslow phase (see text, shown here in row 2) for the NWC phase drift as measured at Dunedin (row 3) between the times of the Onslow and Tumwater (row 1) observations.

Table 3. Calculated Onslow-Tumwater Free-Space Delay Differences[a]

Calculated Phases (µs)	Latitude (deg)	Longitude (deg E.)	Dist. (km)	Delay (µs)
NWC	-21.8163	114.1656		
Tumwater (Pioneer Park)	46.9970	-122.8843	14234.86	47482.4
Onslow	-21.6374	115.1146	100.16	334.1
Δf: Tumwater – Onslow			14134.71	47148.3
Δf: modulo half cycle				1.84
Δo: observed (ex Table 2)				18.4
W/guide delay (Δo – Δf)				16.6

[a]Rows 1–4 show the locations with calculated distances and free space delays for NWC-Tumwater, NWC-Onslow and Onslow-Tumwater. Row 5 then shows the Onslow-Tumwater free-space delay difference modulo half a cycle of 19.8 kHz. This difference is then subtracted from the 18.4 µs observed delay (row 6), from Table 2, to give the waveguide only part of the delay as 16.6 µs (bottom row) which is equivalent to 118°. This observed 118° is then subtracted from the 128° calculated by LWPC for Onslow giving 10° - 180° = -170° which is used, after small seasonal adjustments (see text), in Figure 2c as the 'observed' NWC phase at Tumwater.

Table 4. Comparison of measured long-path H' and β with values from previous measurements and available sources[a]

Data Source (details given in text)	NWC-Tumwater (~14 Mm) H' (km)	NWC-Tumwater (~14 Mm) β (km^{-1})	NPM-Dunedin (~8 Mm) H' (km)	NPM-Dunedin (~8 Mm) β (km^{-1})	NWC-Kauai (~11 Mm) H' (km)	NWC-Kauai (~11 Mm) β (km^{-1})	NLK-Dunedin (~12 Mm) H' (km)	NLK-Dunedin (~12 Mm) β (km^{-1})
Short paths - mid-day Sun all along the path	70.37	0.46	70.55	0.463	70.6	0.485	70.0	0.455
Solar zenith angle adjustment at ends of path	+0.83	-0.04	+0.25	-0.006	+0.55	-0.016	+0.8	-0.02
Results from combining the two rows above	71.2	0.42	70.8	0.46	71.15	0.47	70.8	0.435
Long-path measurements reported here	71.1	0.42	70.8	0.46	71.0	0.46	70.9	(0.38)

[a]The values of H' and β derived from the long-path VLF phase and amplitude measurements reported here are summarized in row 4 for each of the four paths. The corresponding values of H' and β derived from earlier measurements and sources, for constant (mid-day) solar zenith angle along the paths, are shown in row 1. Row 2 shows the adjustments needed for the row 1 values to allow for the higher solar zenith angles towards the ends of the paths. Row 3 combines rows 1 and 2 for comparisons with row 4. (See text for details.)

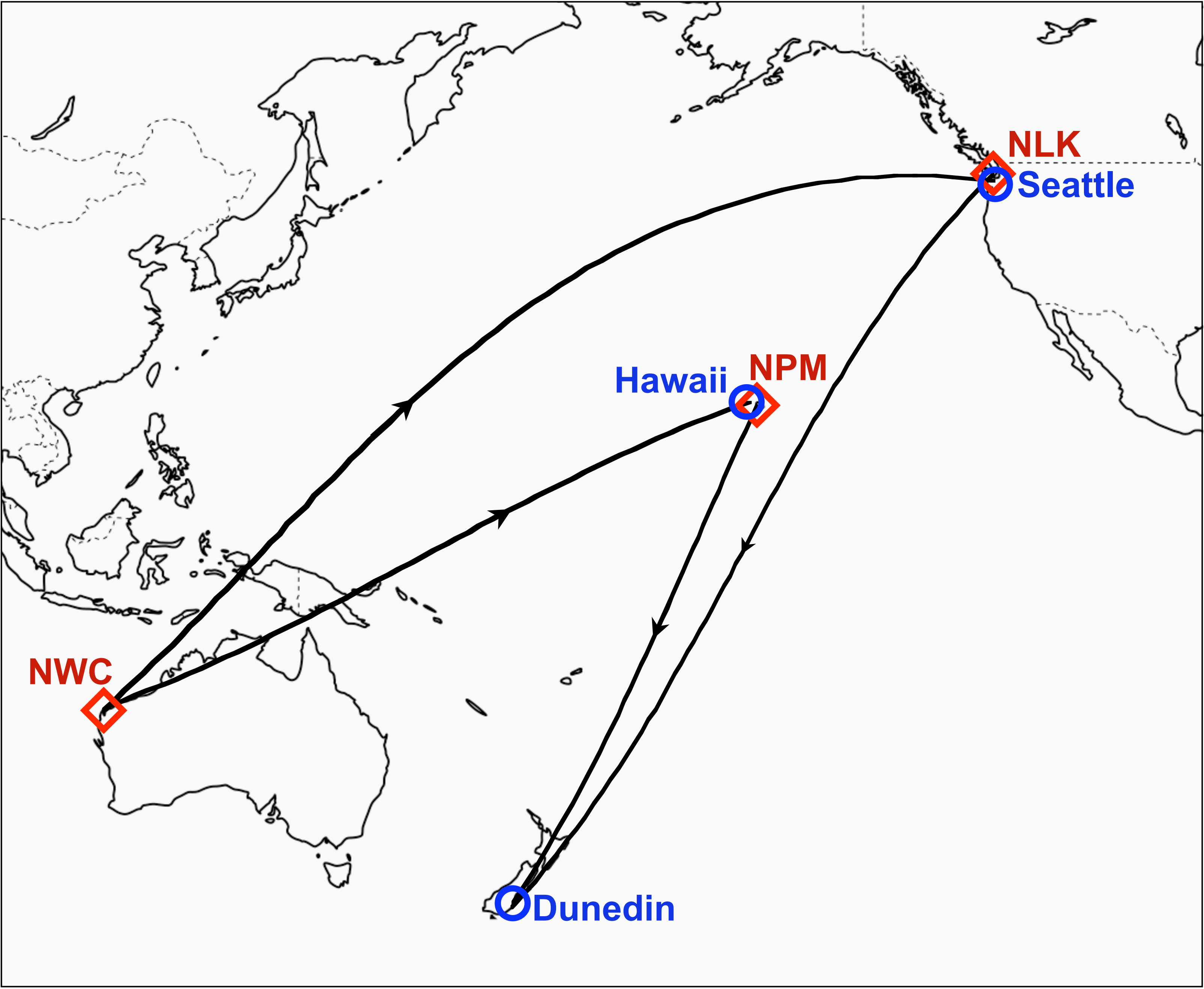
NLK
Seattle
Hawaii
NPM
NWC
Dunedin

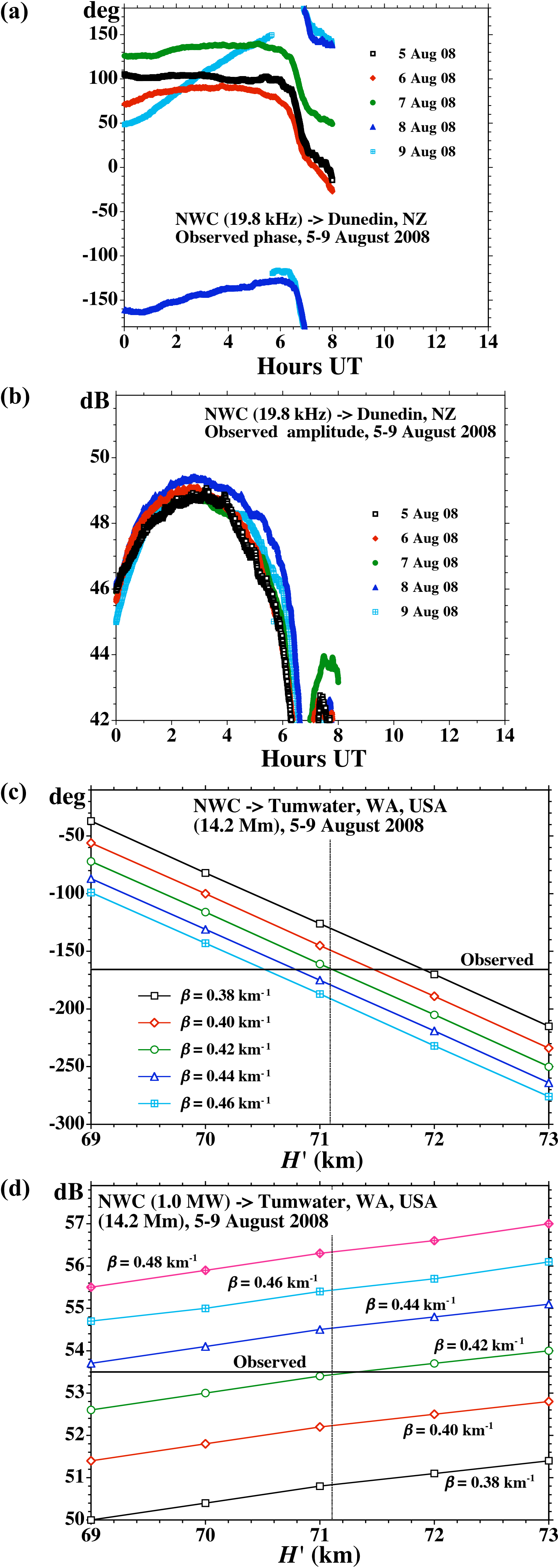
(a)
deg
NWC (19.8 kHz) -> Dunedin, NZ
Observed phase, 5-9 August 2008
5 Aug 08
6 Aug 08
7 Aug 08
8 Aug 08
9 Aug 08
Hours UT
(b)
dB
NWC (19.8 kHz) -> Dunedin, NZ
Observed amplitude, 5-9 August 2008
5 Aug 08
6 Aug 08
7 Aug 08
8 Aug 08
9 Aug 08
Hours UT
(c)
deg
NWC -> Tumwater, WA, USA
(14.2 Mm), 5-9 August 2008
Observed
β = 0.38 km-1
β = 0.40 km-1
β = 0.42 km-1
β = 0.44 km-1
β = 0.46 km-1
H' (km)
(d)
dB
NWC (1.0 MW) -> Tumwater, WA, USA
(14.2 Mm), 5-9 August 2008
β = 0.48 km-1
β = 0.46 km-1
β = 0.44 km-1
β = 0.42 km-1
Observed
β = 0.40 km-1
β = 0.38 km-1
H' (km)

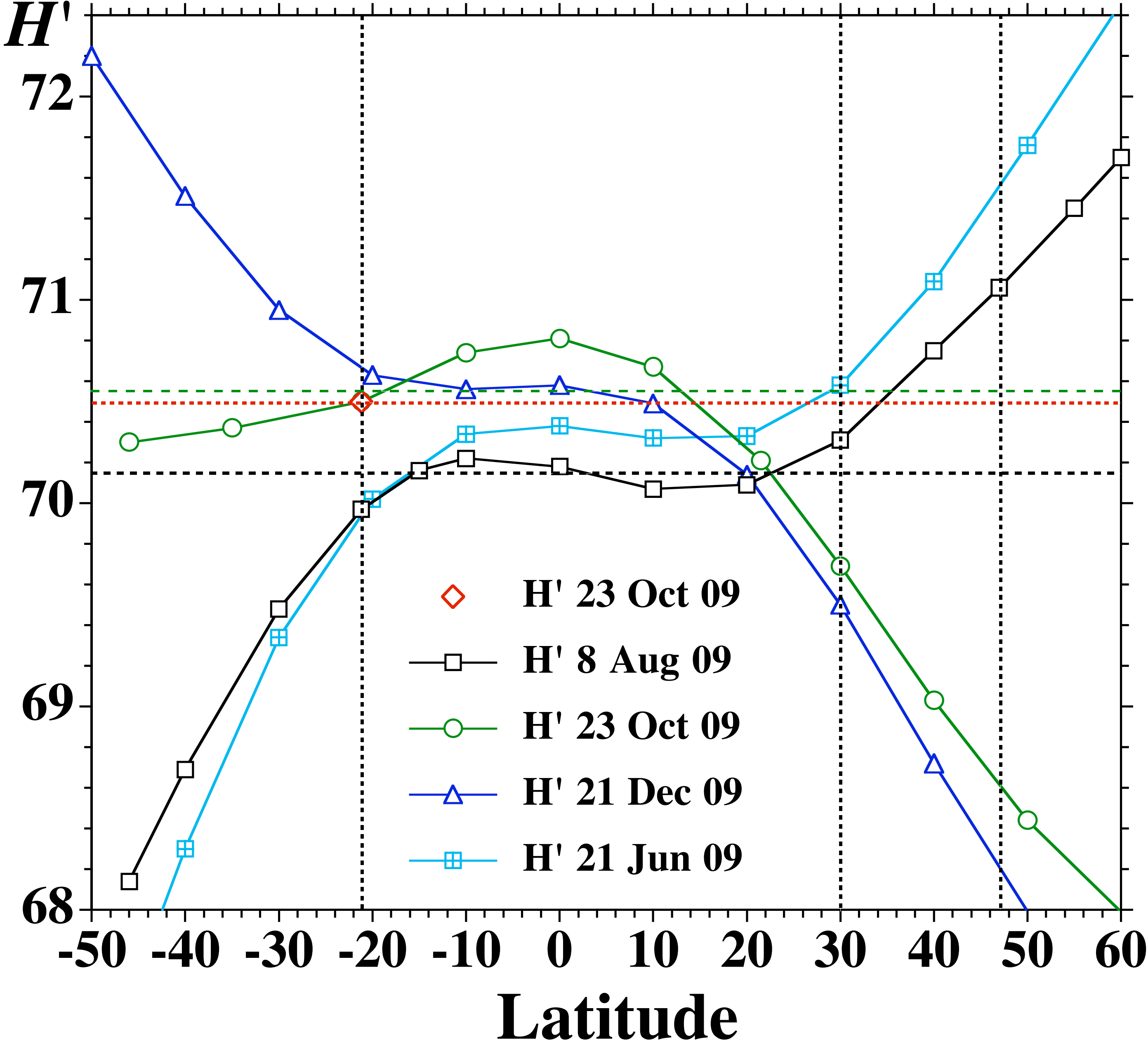

H'
72
71
70
69
68
H' 23 Oct 09
H' 8 Aug 09
H' 23 Oct 09
H' 21 Dec 09
H' 21 Jun 09
-50
-40
-30
-20
-10
0
10
20
30
40
50
60
Latitude

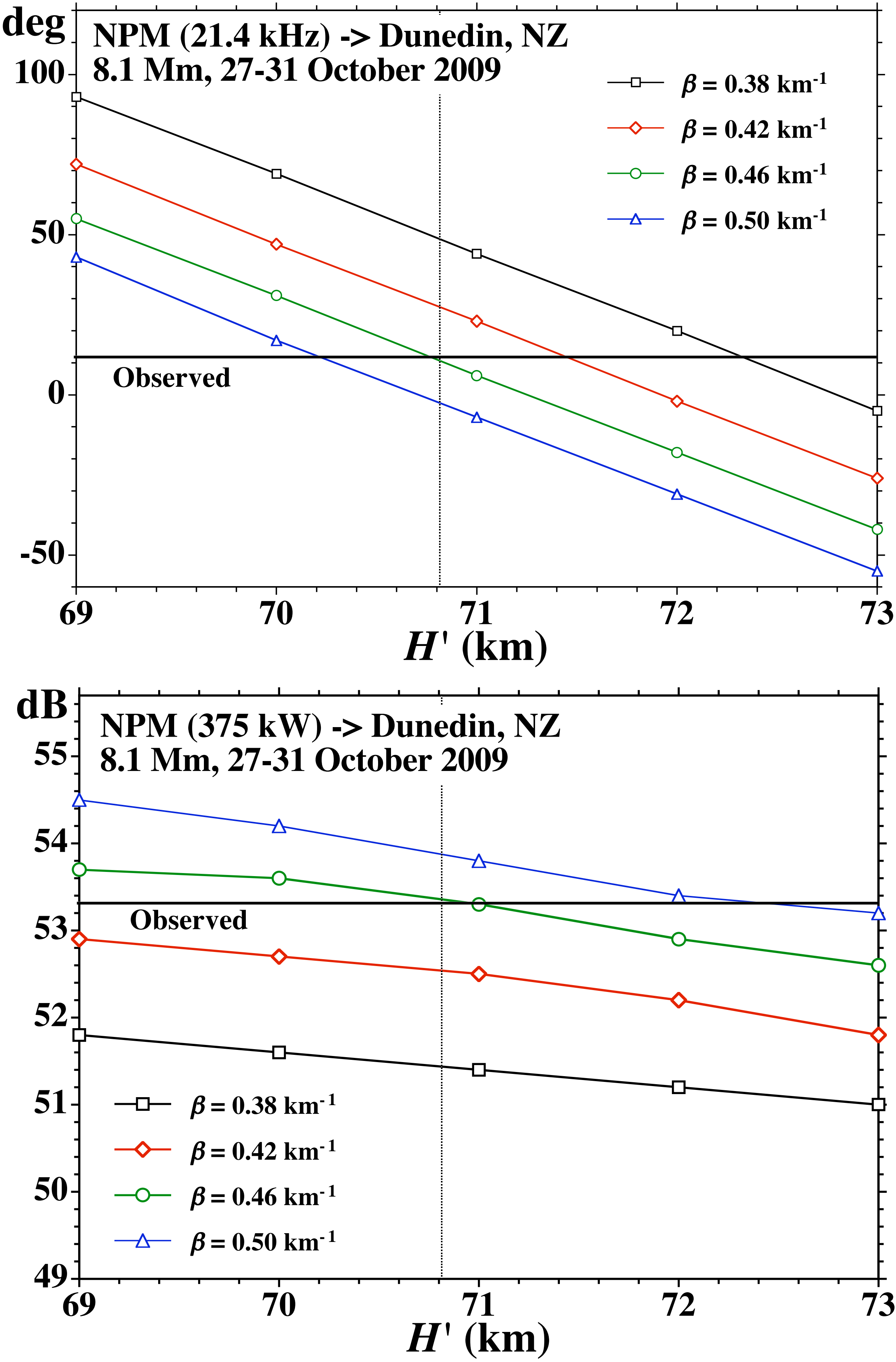
deg
NPM (21.4 kHz) -> Dunedin, NZ
8.1 Mm, 27-31 October 2009
β = 0.38 km-1
β = 0.42 km-1
β = 0.46 km-1
β = 0.50 km-1
Observed
100
50
0
-50
69
70
71
72
73
H' (km)
dB
NPM (375 kW) -> Dunedin, NZ
8.1 Mm, 27-31 October 2009
55
54
53
52
51
50
49
Observed
β = 0.38 km-1
β = 0.42 km-1
β = 0.46 km-1
β = 0.50 km-1
69
70
71
72
73
H' (km)

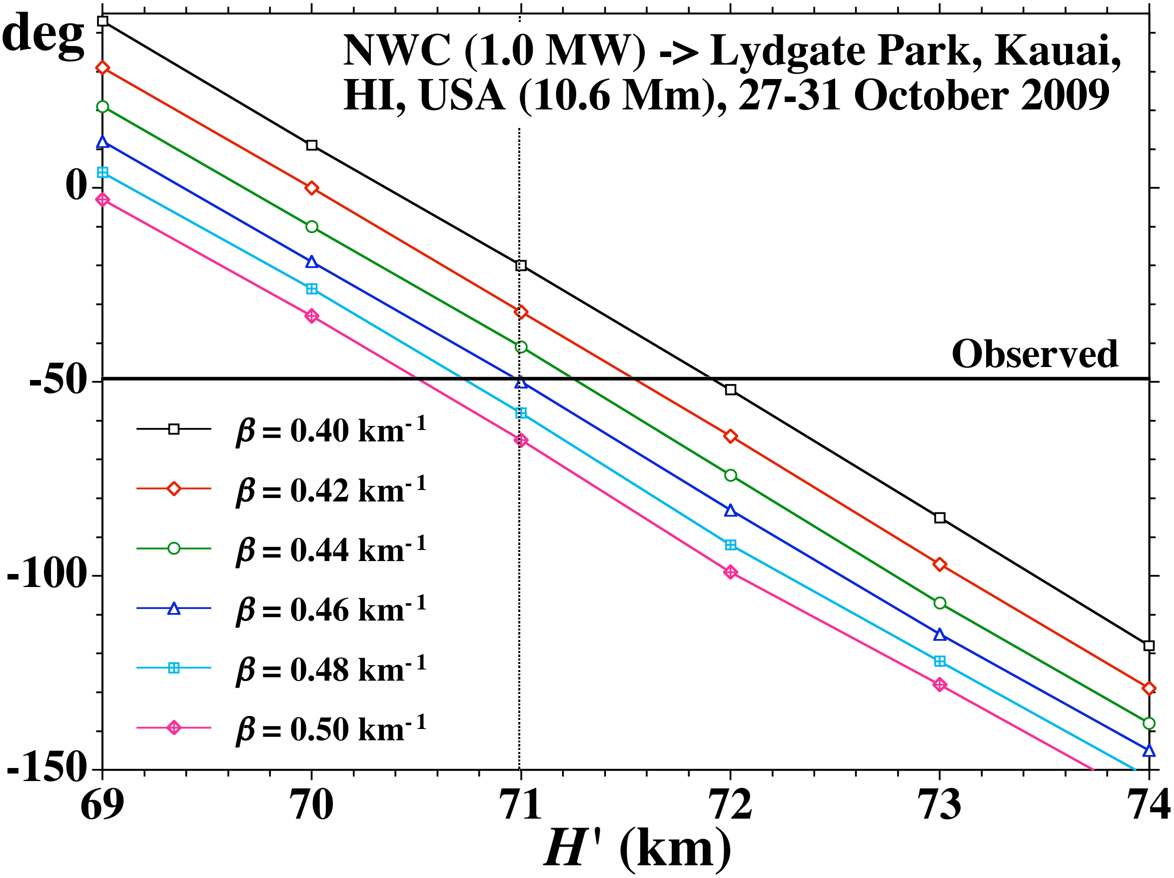
deg
NWC (1.0 MW) -> Lydgate Park, Kauai, HI, USA (10.6 Mm), 27-31 October 2009
Observed
β = 0.40 km-1
β = 0.42 km-1
β = 0.44 km-1
β = 0.46 km-1
β = 0.48 km-1
β = 0.50 km-1
0
-50
-100
-150
69
70
71
72
73
74
H' (km)

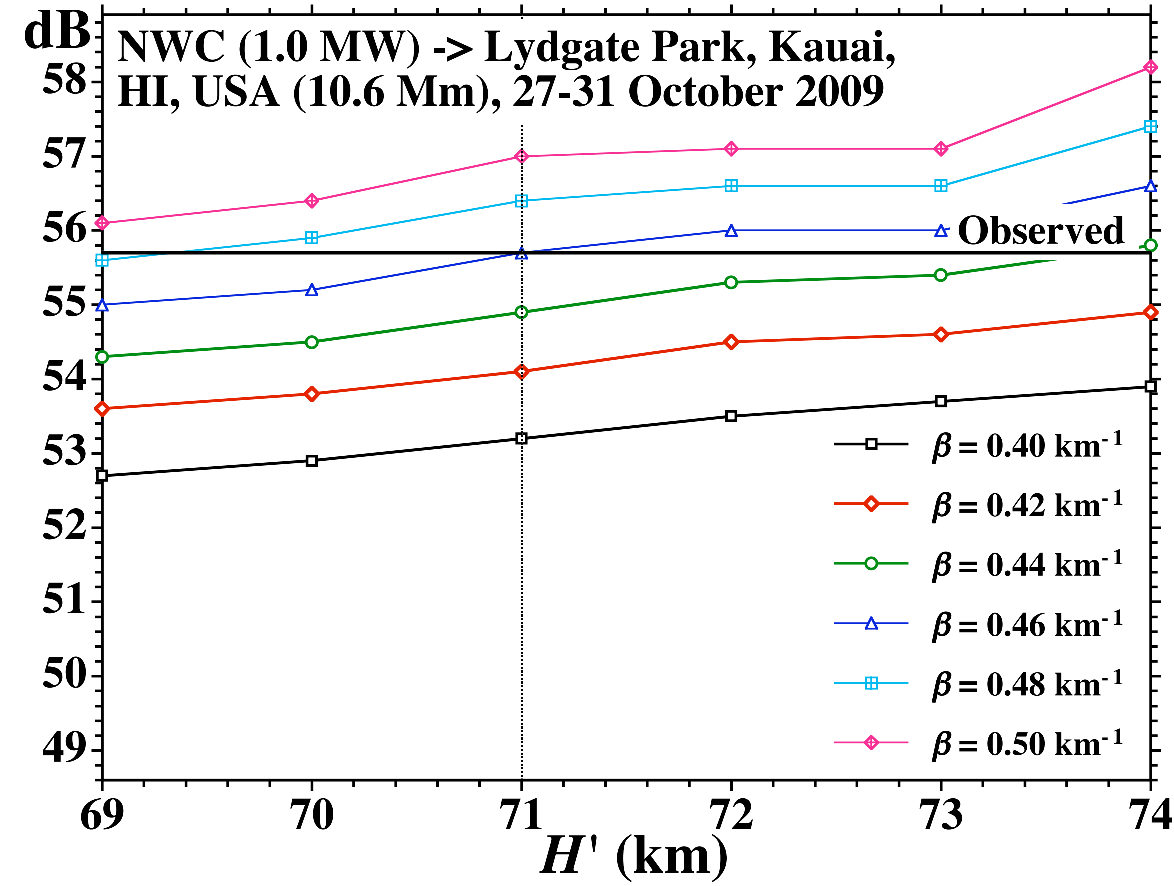
dB
NWC (1.0 MW) -> Lydgate Park, Kauai, HI, USA (10.6 Mm), 27-31 October 2009
Observed
β = 0.40 km-1
β = 0.42 km-1
β = 0.44 km-1
β = 0.46 km-1
β = 0.48 km-1
β = 0.50 km-1
58
57
56
55
54
53
52
51
50
49
69
70
71
72
73
74
H' (km)

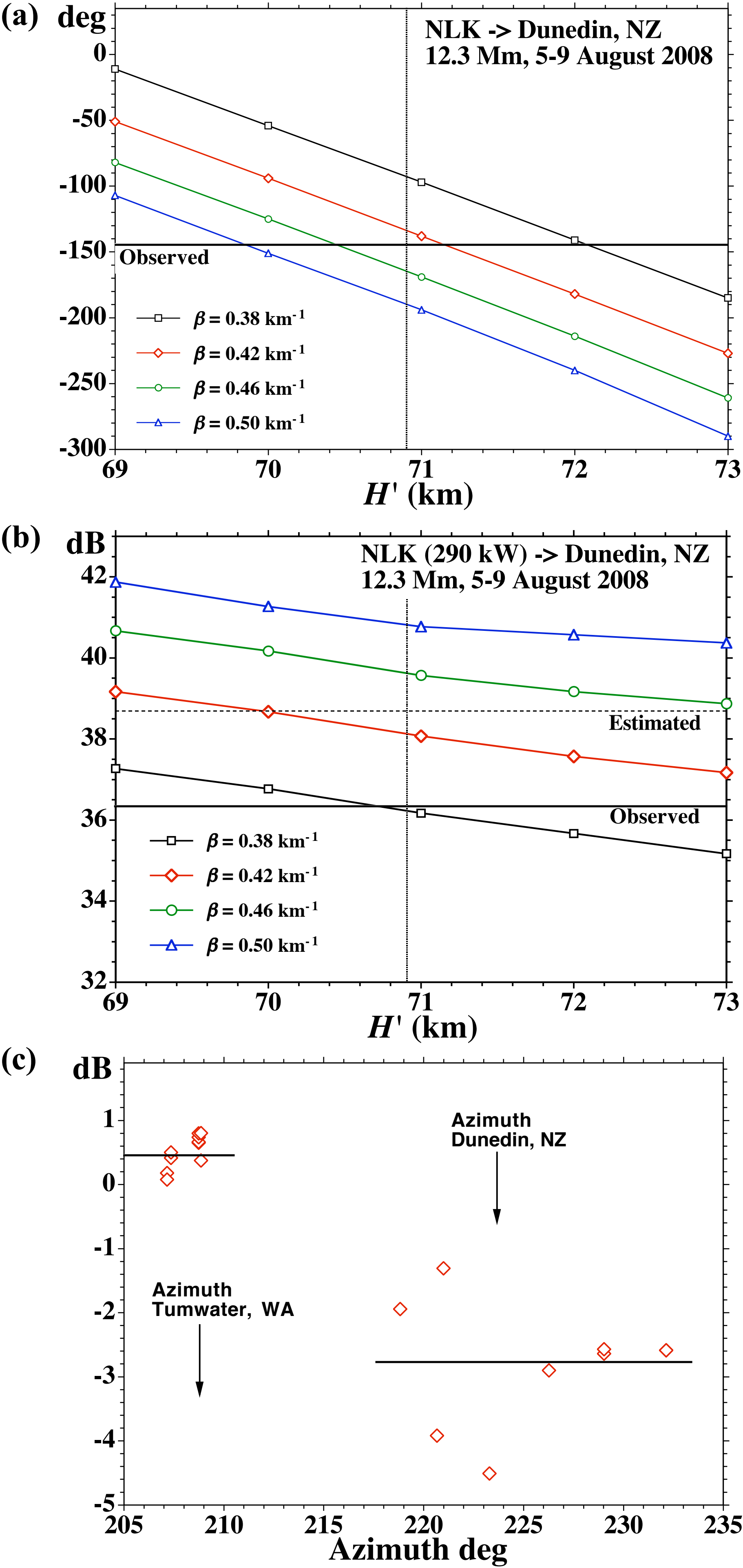

(a)
deg
NLK -> Dunedin, NZ
12.3 Mm, 5-9 August 2008
Observed
β = 0.38 km-1
β = 0.42 km-1
β = 0.46 km-1
β = 0.50 km-1
0
-50
-100
-150
-200
-250
-300
69
70
71
72
73
H' (km)
(b)
dB
NLK (290 kW) -> Dunedin, NZ
12.3 Mm, 5-9 August 2008
Estimated
Observed
β = 0.38 km-1
β = 0.42 km-1
β = 0.46 km-1
β = 0.50 km-1
42
40
38
36
34
32
69
70
71
72
73
H' (km)
(c)
dB
Azimuth
Dunedin, NZ
Azimuth
Tumwater, WA
1
0
-1
-2
-3
-4
-5
205
210
215
220
225
230
235
Azimuth deg